




# Single-Cell Analysis Identifies Distinct Populations of Cytotoxic CD4<sup>+</sup> T Cells Linked to the Therapeutic Efficacy of Immune Checkpoint Inhibitors in Metastatic Renal Cell Carcinoma

Xu Yang <sup>1,\*</sup>, Jianwei Wu <sup>1,\*</sup>, Longlong Fan<sup>2</sup>, Binghua Chen<sup>3</sup>, Shiqiang Zhang<sup>4</sup>, Wenzhong Zheng <sup>1</sup>

<sup>1</sup>Department of Urology, Fujian Medical University Union Hospital, Fuzhou, People's Republic of China; <sup>2</sup>Department of Urology, The Eighth Affiliated Hospital, Sun Yat-sen University, Shenzhen, Guangdong, People's Republic of China; <sup>3</sup>Department of Urology, Pingtan Branch of Fujian Medical University Union Hospital, Fuzhou, People's Republic of China; <sup>4</sup>Department of Urology, Kidney and Urology Center, The Seventh Affiliated Hospital, Sun Yat-sen University, Shenzhen, Guangdong, People's Republic of China

\*These authors contributed equally to this work

Correspondence: Wenzhong Zheng, Department of Urology, Fujian Medical University Union Hospital, 29 Xinquan Road, Gulou District, Fuzhou, Fujian Province, 200001, People's Republic of China, Email wenzhong\_zheng@yeah.net; Shiqiang Zhang, Department of Urology, Kidney and Urology Center, The Seventh Affiliated Hospital, Sun Yat-sen University, 628, Zhenyuan Road, Guangming Dist, Shenzhen, 518107, People's Republic of China, Email zhangshq55@mail.sysu.edu.cn

**Background:** The involvement of cytotoxic CD4<sup>+</sup> T cells (CD4<sup>+</sup> CTLs) and their potential role in dictating the response to immune checkpoint inhibitors (ICIs) in patients with metastatic renal cell carcinoma (mRCC) remains an unexplored area of research.

**Methods:** Utilizing single-cell RNA sequencing, we analyzed the immunophenotype and expression patterns of CD4<sup>+</sup> T lymphocyte subtypes in mRCC patients, followed by preliminary validation via multi-immunofluorescent staining. In addition, we obtained a comprehensive immunotherapy dataset encompassing single-cell RNA sequencing datasets and bulk RNA-seq cohorts from the European Genome-Phenome Archive and ArrayExpress database. Utilizing the CIBERSORTx deconvolution algorithms, we derived a signature score for CD4<sup>+</sup> CTLs from the bulk-RNA-seq datasets of the CheckMate 009/025 clinical trials.

**Results:** Single-cell analysis of CD4<sup>+</sup> T lymphocytes in mRCC reveals several cancer-specific states, including diverse phenotypes of regulatory T cells. Remarkably, we observe that CD4<sup>+</sup> CTLs cells constitute a substantial proportion of all CD4<sup>+</sup> T lymphocyte sub-clusters in mRCC patients, highlighting their potential significance in the disease. Furthermore, within mRCC patients, we identify two distinct cytotoxic states of CD4<sup>+</sup> T cells: CD4<sup>+</sup>GZMK<sup>+</sup> T cells, which exhibit a weaker cytotoxic potential, and CD4<sup>+</sup>GZMB<sup>+</sup> T cells, which demonstrate robust cytotoxic activity. Both regulatory T cells and CD4<sup>+</sup> CTLs originate from proliferating CD4<sup>+</sup> T cells within mRCC tissues. Intriguingly, our trajectory analysis indicates that the weakly cytotoxic CD4<sup>+</sup>GZMK<sup>+</sup> T cells differentiate from their more cytotoxic CD4<sup>+</sup>GZMB<sup>+</sup> counterparts. In comparing patients with lower CD4<sup>+</sup> CTLs levels to those with higher CD4<sup>+</sup> CTLs abundance in the CheckMate 009 and 25 immunotherapy cohorts, the latter group exhibited significantly improved OS and PFS probability.

**Conclusion:** Our study underscores the pivotal role that intratumoral CD4<sup>+</sup> CTLs may play in bolstering anti-tumor immunity, suggesting their potential as a promising biomarker for predicting response to ICIs in patients with mRCC.

**Keywords:** single-cell analysis, granzyme K and granzyme B, cytotoxic CD4<sup>+</sup> T cells, immune checkpoint inhibitors, renal cell carcinoma

## Introduction

In 2021, renal cell carcinoma (RCC) accounted for 2.2% of all newly diagnosed cancer cases worldwide, with a significant toll of 179,368 cancer-related deaths.<sup>1</sup> At diagnosis, approximately one-third of patients newly diagnosed with RCC present with advanced or metastatic disease (mRCC).<sup>2</sup> Furthermore, 30 to 40% of patients who undergo

surgical resection for localized RCC subsequently develop metastatic recurrence, rendering curative-intent surgery unfeasible in these cases.<sup>3</sup>

Immunotherapies have revolutionized the treatment of mRCC, delivering durable responses by harnessing the power of cytotoxic lymphocyte-mediated anti-cancer immunity. Pioneering immunotherapy strategies, such as the use of high-dose interleukin-2 (IL-2), have elicited complete and enduring responses in a subset of mRCC patients, thereby establishing the foundation for the development of modern immunotherapy approaches.<sup>4</sup> In addition, immune checkpoint inhibitors (ICIs), including monoclonal antibodies targeting PD-1/PD-L1 and cytotoxic T-lymphocyte antigen 4 (CTLA-4), have ushered in a paradigm shift in immunotherapy for cancer patients, representing a significant breakthrough in the field.<sup>5,6</sup> In 2015, immune checkpoint inhibitors (ICIs) gained approval from the Food and Drug Administration (FDA) for the treatment of patients with advanced or metastatic renal cell carcinoma (mRCC), following their success in non-small cell lung cancer (NSCLC) and melanoma. Furthermore, nivolumab, a monoclonal anti-PD-1 antibody, has emerged as a promising second-line treatment option for patients with recurrent mRCC.<sup>7</sup> Despite the promise of ICIs in treating advanced or mRCC, only a minority of patients respond favorably to single-agent ICIs, and even initial responders often experience high rates of cancer progression. This limited efficacy may be attributed, in part, to the heterogeneity of intra-tumoral T cells and their differential characteristics in conferring therapeutic benefit upon ICIs treatment.<sup>5,8</sup>

PD-1/PD-L1 monoclonal antibodies trigger anti-tumor responses by disrupting adaptive immune resistance mechanisms. Presently, CD8<sup>+</sup> T lymphocytes are at the forefront of investigations aiming to understand how immune-checkpoint inhibitors stimulate anti-tumor immunity.<sup>9</sup> In melanoma patients, the abundance of CD8<sup>+</sup> T lymphocytes at the tumor-invasive margin is strongly correlated with the subsequent response to ICIs directed therapy, suggesting a potential predictive biomarker for treatment efficacy.<sup>9,10</sup>

Despite the notable infiltration of CD8<sup>+</sup> T lymphocytes in RCC, contrary to many other cancer types, this infiltration does not necessarily translate into improved treatment responses or prognosis.<sup>11</sup> Intriguingly, a recent study reveals that nivolumab, an immune checkpoint inhibitor, binds pre-expanded CD8<sup>+</sup> T cells in responder patients with metastatic renal cell carcinoma (mRCC), leading to the upregulation of granzyme family proteases (granzyme K and B) with cytotoxic potential.<sup>12</sup> However, the significance of heterogeneous subsets of tumor-infiltrating T lymphocytes in RCC, beyond the canonical CD8<sup>+</sup> exhausted and cytotoxic phenotypes, in response to immune checkpoint inhibitors remains largely unexplored. Specifically, the role of CD4<sup>+</sup> T lymphocytes in either enhancing or controlling RCC cancer growth is still poorly understood.

The efficacy of T lymphocyte-mediated immunity relies on the recognition of antigens by CD8<sup>+</sup> and CD4<sup>+</sup> T cells, within the context of major histocompatibility complex class I (MHC-I) and MHC-II molecules, respectively. Notably, in a distinct Phase II clinical trial involving melanoma patients, the response rate to anti-PD-1 therapy was linked to elevated MHC-II molecule expression and IFN- $\gamma$ -related signaling prior to treatment.<sup>13</sup> Within the complex cancer microenvironment, the diverse functional polarization of CD4<sup>+</sup> T lymphocytes, encompassing T helper cells (Th1, Th2, and Th17) and regulatory CD4<sup>+</sup> T cells (Tregs), has been incontrovertibly demonstrated to exert distinct effects on cancer immunity.<sup>14–17</sup> The direct cytolytic prowess of CD4<sup>+</sup> T cells against cancer in select patient populations has garnered significant attention in recent studies.<sup>18,19</sup> Specifically, cytotoxic CD4<sup>+</sup> T cells (CD4<sup>+</sup> CTLs) were initially identified in individuals with B-cell chronic lymphocytic leukemia, and their antitumor capabilities were subsequently validated in melanoma patients undergoing anti-CTLA-4 therapy.<sup>20,21</sup> Extensive research has further revealed that antigen-specific CD4<sup>+</sup> CTLs recognize autologous melanoma cell lines and efficiently eliminate targeted cells in an MHC-II-dependent manner.<sup>21</sup> Notably, a recent study demonstrated that bladder cancer harbors diverse CD4<sup>+</sup> CTL states, which possess the capacity to lyse autologous cancer cells through MHC-II-mediated interactions. Interestingly, these processes can be modulated by autologous Tregs.<sup>22</sup> Furthermore, when comparing patients treated with anti-PD-L1 for bladder cancer (IMvigor210 cohort), responders exhibited significantly higher CD4<sup>+</sup> CTL-specific signatures compared to non-responders, suggesting a potential role of these cells in immunotherapy response.<sup>22</sup> Despite the elucidation of anticancer mechanisms and functional regulation of CD4<sup>+</sup> CTLs across various cancer types, the existence of these cells and their potential role in modulating the response to ICIs in mRCC patients has yet to be reported. A thorough characterization of CD4<sup>+</sup> CTL subsets within the tumor microenvironment is imperative to precisely map the immunogenic cells responsible

for anticancer immunity and to establish predictive biomarkers that can guide treatment decisions for ICIs in RCC patients.

In this study, we undertook a comprehensive evaluation of CD4<sup>+</sup> T cell subtypes and examined their association with the response to ICIs in mRCC patients. Leveraging published single-cell RNA sequencing data targeting CD4<sup>+</sup> T cells, we analyzed the expression profile and functional characteristics of CD4<sup>+</sup> CTLs in RCC samples.<sup>23</sup> Additionally, we employed multiple immunofluorescent staining techniques to validate the expression patterns and phenotypic states of CD4<sup>+</sup> CTLs in RCC tissues. To assess the synergistic role of CD4<sup>+</sup> CTLs in predicting ICIs response, we analyzed immunotherapy datasets from mRCC patients, including an independent single-cell RNA sequencing dataset and a bulk RNA-seq cohort. Collectively, these findings provide a profound characterization of tumor-specific CD4<sup>+</sup> CTLs in cancer and identify a promising marker for predicting effective ICIs response in mRCC patients.

## Materials and Methods

### Acquisition of the Single-Cell RNA Sequencing, Bulk RNA-Seq and Microarray Data

Utilizing the accession number GSE156728 ([Supplementary Table 1](#)),<sup>23</sup> we downloaded single-cell RNA sequencing data targeting tumor-infiltrating CD4<sup>+</sup> T cells from six mRCC and paired normal tissues from the Gene Expression Omnibus (GEO) database. This dataset enabled us to analyze the expression patterns and functional status of CD4<sup>+</sup> CTLs. Two independent single-cell RNA sequencing datasets of mRCC patients treated with anti-PD-1 therapy were downloaded to evaluate the synergistic role of CD4<sup>+</sup> CTLs in predicting ICIs response. These datasets were obtained from the European Genome phenome Archive (EGA, accession number EGAD00001008166) and the Single Cell Portal database (SCP, accession number SCP1288).<sup>12,24</sup> In the EGAD00001008166 dataset, CD4<sup>+</sup> T lymphocytes were isolated from two RCC patients, one responder and one non-responder, following ICIs treatment.<sup>12</sup> Regarding the SCP1288 dataset, tumor-infiltrating CD45<sup>+</sup> leukocytes were obtained from two mRCC patients, before and after exposure to ICIs.<sup>24</sup> To validate the CD4<sup>+</sup> CTL signature in unpaired RCC samples, we accessed the CheckMate 009 cohort from the ArrayExpress database, comprising pre- and on-therapy microarray data of 57 patients treated with anti-PD-1 (nivolumab) therapy (accession number E-MTAB-3218). This dataset was based on the Affymetrix Human Genome U219 Array platform. In the present study, we employed the RMA (robust multiarray average) method, utilizing the Affy and sva packages in R software, to preprocess the E-MTAB-3218 microarray data. This preprocessing involved background subtraction, quantile normalization, and the calculation of average gene expression values. Besides, the Checkmate 010 and Checkmate 025 cohorts, including processed bulk transcriptomes data and paired clinical information, were downloaded from Braun's and David's studies.<sup>25,26</sup> The Checkmate 010 cohort was a clinical phase II dose-finding study of anti-PD-1 therapy (nivolumab), demonstrating no correlation between dose-dependency and progression-free survival (PFS) in patients with mRCC.<sup>27</sup> Whereas, the Checkmate 025 cohort was a randomized clinical Phase III trial that demonstrated an improvement in overall survival with anti-PD-1 therapy (nivolumab) compared to the mTOR inhibitor (everolimus).<sup>5</sup>

### Single-Cell RNA Sequencing Data Processing and Cell Type Determination

Utilizing the CellRanger software (Version 6.0), we generated precise raw read count matrices from single-cell RNA sequencing data. Subsequently, to facilitate downstream analysis, we employed the Seurat (Version 4.1.0) package in the R statistical programming language software to transform these matrices into the standardized Seurat object format. The tumor-infiltrating immune cells were stringently evaluated and prioritized based on their corresponding barcode numbers. Cells harboring either a mitochondrial genome-associated molecular identifier fraction exceeding 15% or a gene count below 300 were rigorously excluded from further analysis. Subsequently, a negative binomial regression model within the SCTransform function was precisely implemented to normalize the total read counts of the retained immune cells, ensuring data consistency and reliability for downstream applications.<sup>28</sup> Furthermore, to mitigate potential biases introduced by cell cycle variations, the read count matrices underwent normalization using the CellCycleScoring function, effectively diminishing the influence of cell cycle phase. To address the batch effect observed among RCC samples, we applied the Harmony method, ensuring the comparability of data across batches. Additionally, we calculated the principal components of the expression matrices utilizing the RunPCA function, capturing the underlying biological

variations. Subsequently, we employed the FindClusters function to identify distinct cell clusters within the data, which were further visualized using the RunUMAP function, providing a comprehensive overview of the cellular landscape. Finally, we leveraged the FindMarkers function to pinpoint differentially expressed genes (DEGs) between each cell cluster, revealing key molecular signatures that characterize these subpopulations.

## Differential Expression Gene Analysis and function Annotation Analysis

To assess the immune-related status (IRs) of individual CD4<sup>+</sup> T cells in mRCC samples, we curated four immune regulation and attack-associated gene sets from the Molecular Signatures Database (MSigDB), including GO\_BP\_T\_CELL\_TOLERANCE, GO\_BP\_T\_CELL\_HOMEOSTASIS, GO\_BP\_T\_CELL\_MEDIATED\_CYTOTOXICITY, and GO\_BP\_CYTOLYSIS. The AUCell R package (Version 1.19.1) was utilized to compute the area under the curve (AUC) value for each cell, based on these four IRs-related gene sets. This AUC score serves as a metric to estimate and rank the proportion of genes within the IRs-related gene sets that are highly expressed in each cell. Utilizing the AUCell\_exploreThresholds function, we calculated an optimal threshold to identify cells with an active gene set. Subsequently, cell clusters were color-coded based on the ranked AUC scores of individual cells, enabling us to visualize which clusters exhibit activation in the IRs gene set. To gain further insights into the potential functions of CD4<sup>+</sup> T lymphocyte subsets, we performed functional annotation analyses on the differentially expressed genes (DEGs) of identified cell clusters. Specifically, we employed the ClusterProfiler (Version 4.5.2) and org.Hs.eg.db (Version 3.15.0) packages in R software to conduct gene ontology (GO) and Kyoto Encyclopedia of Genes and Genomes (KEGG) pathway enrichment analyses. Additionally, we utilized gene set enrichment analysis (GSEA) with the ClusterProfiler and org.Hs.eg.db packages to compare the immune activation status between two distinct cell subsets. For all analyses in this section, a p-value less than 0.05 was deemed statistically significant, ensuring rigorous and reliable results.

## Biopsy Collection and Immunofluorescent Staining

RCC samples were acquired from 20 patients undergoing nephrectomy or nephron-sparing surgery between 2021 and 2022 at Fujian Medical University Union Hospital and Seventh Affiliated Hospital of Sun Yat-sen University. Written informed consent was obtained from 20 RCC patients respectively, and the present research received institutional review board approval from Fujian Medical University Union Hospital and Seventh Affiliated Hospital of Sun Yat-sen University research ethics committee according to Helsinki declaration (Ethics number 2024KJT043). Biopsies were fixed by bouin's fixative and further embedded in paraffin for multiple immunofluorescent staining study. Primary antibody including CD4 (Cat#AF-379-SP, RRID:AB\_394582, NOVUS), GZMK (Cat#67272-1-Ig, RRID:AB\_1294297, Proteintech) and GZMB (Cat#ab243879, RRID:AB\_2819068, Abcam) were used to immunofluorescence staining. In this study, we performed CD4<sup>+</sup>GZMK<sup>+</sup>GZMB multiple fluorescence staining protocol. Specifically, 5µm paraffin slides of RCC biopsies were repeat deparaffinized twice in dimethylbenzene solution and further rehydrated in alcohol solution including 100%, 95%, 85% and 70% respectively. After PBS washing, antigen retrieval was performed by Tris-EDTA (TE, pH = 9.0) solution. Then, endogenous peroxidase was inactivated in H<sub>2</sub>O<sub>2</sub> solution, and nonspecific binding effects including primary and secondary antibodies was removed by using 8% bovine serum albumin at room temperature for 45 min. Subsequently, samples were incubated with primary antibodies including CD4, GZMK and GZMB at an optimal dilutions (1:100, 1:200 and 1:400 respectively). After incubate overnight in 4 °C refrigerator and PBS washing, RCC samples were incubated with corresponding fluorescent secondary antibody at a 37 °C thermostat for 45 min. Finally, nucleuses were mounted with DAPI (2-(4-Amidinophenyl)-6-indolecarbamide dihydrochloride) (Cat#P0131, Beyotime Biotechnology). Corresponding isotype of primary antibodies were served as negative controls during the procedure of staining (data not shown).

## Characterization of Cell-Type Infiltration Based on Single-Cell Expression Matrix

To estimate the the proportions of identified cell types from bulk transcriptomes data, we used a website based tool CIBERSORTx<sup>29</sup> (<https://cibersortx.stanford.edu/>) to generate a reference signature matrix from single-cell RNA sequencing dataset (GSE156728) and calculate CD4<sup>+</sup> CTLs and related subdivided cell types proportions from microarray and bulk RNA-seq datasets based established cell-type reference. Specifically, we ran the "Create Signature



Matrix” module of CIBERSORTx to generate reference single-cell RNA sequencing signature matrix. Then, we performed CIBERSORTx deconvolution on bulk transcriptomes datasets including, Checkmate 010, and Checkmate 025 cohort based on the generated reference single-cell RNA sequencing signature matrix. In this study, related parameters are kept at CIBERSORTx online tool default settings and samples with p value less than 0.05 were selected for further study.

## CytoTRACE Differentiation States and Pseudotime Trajectory Analysis

In order to reveal the differentiation states of CD4<sup>+</sup> T cells in RCC, we used CytoTRACE (Version 0.3.3), a robust computational framework R package developed for differentiation states and stemness status prediction via single-cell RNA sequencing data.<sup>30</sup> The cells in GSE156728 dataset including proliferating CD4<sup>+</sup> T cells (regulatory Treg\_PROLIF and cytotoxic CD4\_CTL\_PROLIF), regulatory T cells (Treg\_HSPA1A and Treg\_LAYN) and cytotoxic CD4<sup>+</sup> T cells (CD4\_GZMB and CD4\_GZMK) were obtained a CytoTRACE score according to their differentiation characteristics, with a lower score indicating higher differential states. In addition, we performed pseudotime analysis based on Monocle (Version 2.10.1) R package<sup>31</sup> to map cytotoxic CD4<sup>+</sup> T cells differentiation trajectory with num\_cells\_expressed  $\geq 10$ , mean expression  $\geq 0.125$  and qval  $< 0.01$  in GSE156728 RCC patients. Meanwhile, branched expression analysis modeling (BEAM) algorithm in Monocle package was used to identify branch-drive genes followed by unbiased clustering of genes based on the patterns of co-expression in specific branches identified from pseudotime trajectory analysis.

## Statistical Analysis

In this study, measurement data pertaining to continuously varying variables were expressed as either median  $\pm$  quartiles (Q) or mean  $\pm$  standard deviation (SD), depending on the distribution characteristics of the variables, which were assessed using the Shapiro–Wilk test for normality or skewness. Conversely, categorical variables related to enumeration data were reported as frequencies (proportions). To compare the ICI response and no-response groups, statistical analyses were conducted using the Mann–Whitney *U*-test for median  $\pm$  quartiles (Q) data, two independent samples *t*-test for mean  $\pm$  standard deviation (SD) data, and Chi-square or Fisher’s exact test for frequencies and proportions data. The prognostic implications of CD4<sup>+</sup> CTLs in RCC patients, specifically their impact on overall survival (OS) and progression-free survival (PFS), were comprehensively assessed using Kaplan–Meier (KM) curves implemented in R software (utilizing the survminer and survival packages). To facilitate this analysis, patients were stratified based on the median abundance of CD4<sup>+</sup> CTLs, distinguishing between those with high and low abundance. Log rank tests were then employed to compare the survival curves between these groups, enabling us to statistically evaluate the significance of any observed differences in survival. Given the non-normal distribution of CD4<sup>+</sup> CTLs expression levels within the small cohort of renal cancer patients included in this study, the Mann–Whitney *U*-test was deemed appropriate for analyzing the differences in CD4<sup>+</sup> CTLs expression between various immune checkpoint inhibitor (ICI) response groups. In this study, all statistical analysis were performed in R software (Version 4.2.1, Microsoft, Redmond, WA) and p value less than 0.05 (two paired manner) was set as statistically significant level.

## Results

### CD4<sup>+</sup> T Lymphocytes Include Regulatory and Cytotoxic States That are Enriched in Renal Cell Carcinoma

To gain insights into the composition of CD4<sup>+</sup> T lymphocytes within the tumor microenvironment, we conducted a comprehensive analysis of a single-cell RNA sequencing dataset targeting tumor-infiltrating CD4<sup>+</sup> T cells. This dataset encompassed six renal cancer samples and their adjacent uninvolved kidney tissues. Following stringent quality control measures, 10,105 CD4<sup>+</sup> tumor-infiltrating T cells were selected for further investigation. Notably, the sequencing saturation rate exceeded 85%, and each individual CD4<sup>+</sup> T cell exhibited 24,148 unique features. Leveraging uniform manifold approximation projection (UMAP) and cell marker gene analysis, we preliminarily identified four distinct cell states within the RCC tissues, as depicted in Figure 1A.

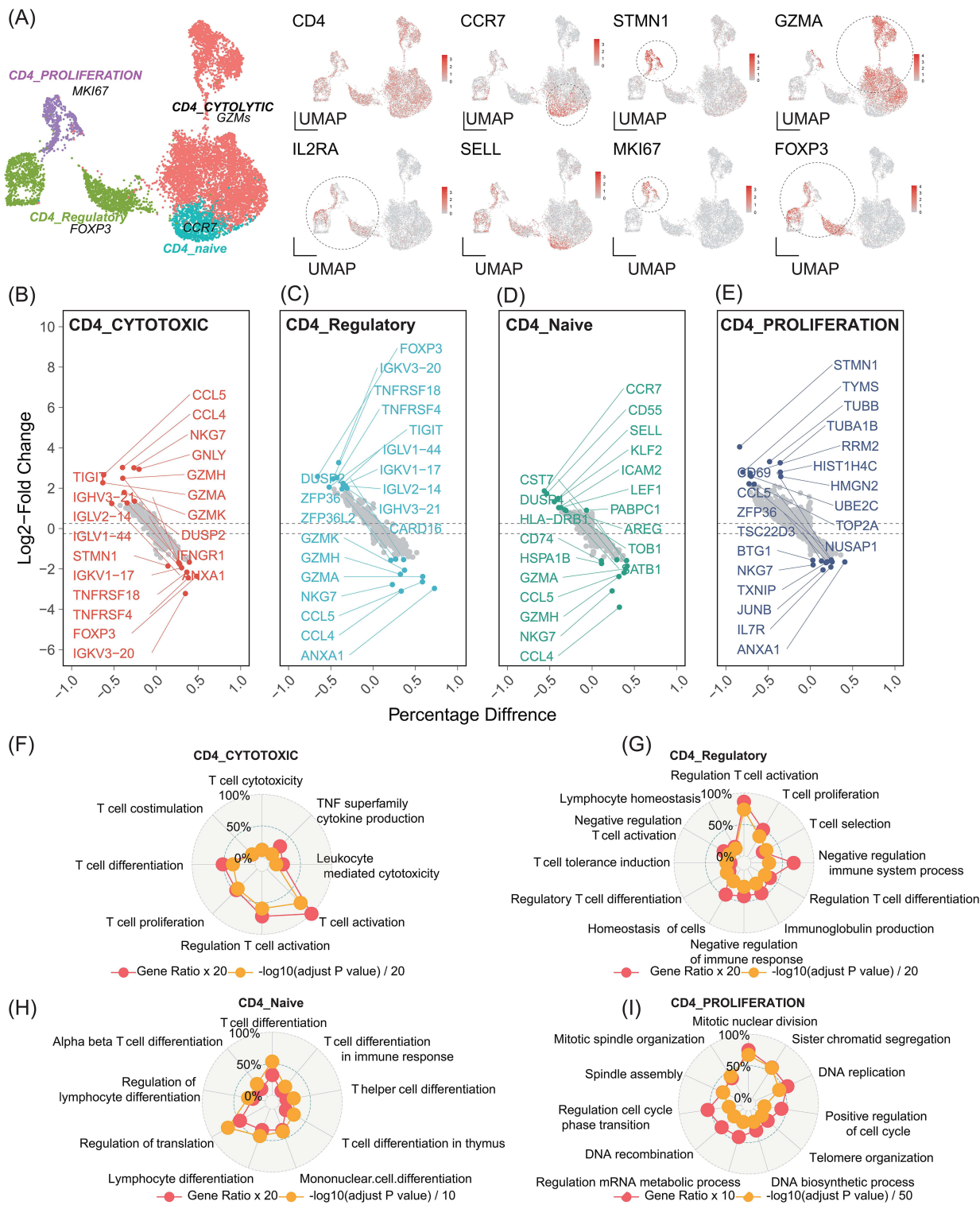


**Figure 1** CD4+ T cells encompass cytotoxic and regulatory states that are enriched in the environment of metastatic renal cell carcinoma. **(A)** Uniform Manifold Approximation and Projection (UMAP) visualization along with cell marker gene analysis of single-cell RNA sequencing data from metastatic renal cell carcinoma. Each dot represents a single cell and is colored according to its respective cluster. Specifically, MKI67 identifies the CD4\_PROLIFERATION cell cluster, CCR7 marks the CD4\_naive cell cluster, FOXP3 represents the CD4\_Regulatory cell cluster, and GZMs designate the CD4\_CYTOTOXIC cell cluster; **(B–E)** Differentially expressed genes were identified between each cell cluster, including the CD4\_CYTOTOXIC, CD4\_PROLIFERATION, CD4\_Regulatory, and CD4\_naive clusters. CD4\_CYTOTOXIC versus other cell clusters **(B)**; CD4\_Regulatory versus other cell clusters **(C)**; CD4\_naive versus other cell clusters **(D)**; CD4\_PROLIFERATION versus other cell clusters **(E)**; The CD4\_CYTOTOXIC cluster was enriched in pathways pertaining to T cell cytotoxicity **(F)**. Conversely, the CD4\_Regulatory cluster was enriched in pathways that promote T cell tolerance induction **(G)**. The CD4\_naive cell cluster was associated with cell differentiation processes, including T cell differentiation **(H)**. Finally, the CD4\_PROLIFERATION signature exhibited a pronounced mitotic nuclear division and cell proliferation **(I)**.

In this study, we annotated cell states or clusters based on the expression of cell marker genes derived from published literature. Specifically, one cell cluster exhibited high expression of IL2RA (Interleukin 2 Receptor Alpha Subunit), TIGIT (T-cell Immunoreceptor with Ig and ITIM Domains), and FOXP3 (Forkhead Box P3), indicating its identity as a *CD4\_Regulatory* cell cluster, comprising 2036 cells (Figure 1A). Another cluster displayed elevated levels of genes associated with memory functions, including CCR7 (Chemokine Receptor 7), IL-7R (Interleukin 7 Receptor), and SELL (Selectin L), thus representing a *CD4\_Naive* cell cluster with 1067 cells (Figure 1A). A third cluster was enriched in proliferation-linked genes, such as ZWINT (ZW10 Interacting Kinetochose Protein), MKI67 (Marker of Proliferation Ki-67), and TYMS (Thymidylate Synthetase), designated as the *CD4\_PROLIFERATION* cell cluster, consisting of 595 cells (Figure 1A). Finally, the fourth cluster displayed high expression of cytolytic function-related genes, including GZMA (Granzyme A), GZMH (Granzyme H), and NR4A2 (Nuclear Receptor Subfamily 4 Group A Member 2), identifying it as the *CD4\_CYTOTOXIC* cell cluster, comprising 6407 cells (Figure 1A).

We conducted differential gene expression (DEGs) analysis to identify distinguishing genes within the respective cell clusters. In comparison to the *CD4\_Regulatory*, *CD4\_Naive*, and *CD4\_PROLIFERATION* clusters, the *CD4\_CYTOTOXIC* cell cluster displayed elevated expression of cytotoxic lineage genes, encompassing GZMA (Granzyme A), GZMK (Granzyme K), GZMB (Granzyme B), GZMH (Granzyme H), NKG7 (Natural Killer Cell Granule Protein 7), GNLY (Granulysin), and PRF1 (Perforin 1). Conversely, this cluster exhibited reduced expression of regulatory genes, such as FOXP3, TIGIT, IGKV1-17 (Immunoglobulin Kappa Variable 1–17), IGKV3-20 (Immunoglobulin Kappa Variable 3–20), IGLV2-14 (Immunoglobulin Lambda Variable 2–14), IGLV1-44 (Immunoglobulin Lambda Variable 1–44), and IGHV3-21 (Immunoglobulin Heavy Variable 3–21) (Figure 1B). In stark contrast to the *CD4\_CYTOTOXIC* cluster, the *CD4\_Regulatory* cluster exhibits robust expression of regulatory genes, including FOXP3, TIGIT, IGKV3-20, IGKV1-17, IGLV2-14, and IGHV3-21. Conversely, it displays significantly lower expression levels of cytotoxic factors, such as GZMK, GZMH, GZMA, and NKG7 (Figure 1C).

The *CD4\_Naive* cell clusters exhibit a higher expression of CCR7 and SELL, both serving as widely recognized markers for distinguishing between naive and memory cells (Figure 1D). Similarly, *CD4\_PROLIFERATION* cell cluster highly express some proliferation-related genes, such as STMN1 and TYMS (Figure 1E).

Furthermore, to validate the functional roles of  $CD4^+$  T cell subsets in renal cell carcinoma (RCC) patients, we conducted a comprehensive function annotation analysis leveraging the differentially expressed genes (DEGs) in the respective cell clusters. Notably, the DEGs in the *CD4\_CYTOTOXIC* cluster were predominantly enriched in pathways associated with T cell cytotoxicity, leukocyte cytotoxicity, T cell activation, T cell proliferation, T cell co-stimulation, and TNF super-family cytokine production. These findings provide further evidence of the *CD4\_CYTOTOXIC* cluster's specialized functions in mediating cytotoxic responses in RCC patients (Figure 1F). The signature of the *CD4\_Regulatory* cluster revealed enrichment in pathways that promote T cell tolerance induction, regulatory T cell differentiation, lymphocyte homeostasis, immunoglobulin production, as well as negative regulation of T cell activation and immune response (Figure 1G). The signature genes within the *CD4\_Naive* cluster were intricately linked to cell differentiation processes, encompassing T cell differentiation, T cell differentiation in immune response, T helper cell differentiation, T cell differentiation in the thymus, lymphocyte differentiation, alpha-beta T cell differentiation, and regulation of cell translation (Figure 1H). The *CD4\_PROLIFERATION* cluster, on the other hand, exhibited a distinct signature that was predominantly associated with cell cycle and division. This signature encompassed processes such as mitotic nuclear division, sister chromatid segregation, mitotic spindle organization, spindle assembly, DNA replication, regulation of cell cycle phase transition, DNA recombination, telomere organization, and DNA biosynthetic processes (Figure 1I). These data indicate that the *CD4\_PROLIFERATION* cluster comprises actively proliferating T cells.

To delve deeper into the functional disparities between the *CD4\_CYTOTOXIC* and *CD4\_Regulatory* cell clusters, we employed Gene Set Enrichment Analysis (GSEA) to uncover the altered pathways between these two clusters. Notably, our analysis revealed that the *CD4\_CYTOTOXIC* cluster exhibited enrichment in immune activation pathways (Figure 2A). This finding, coupled with our previous function annotation analysis, further substantiates the distinct and specialized roles played by these  $CD4^+$  T cell clusters in RCC patients.

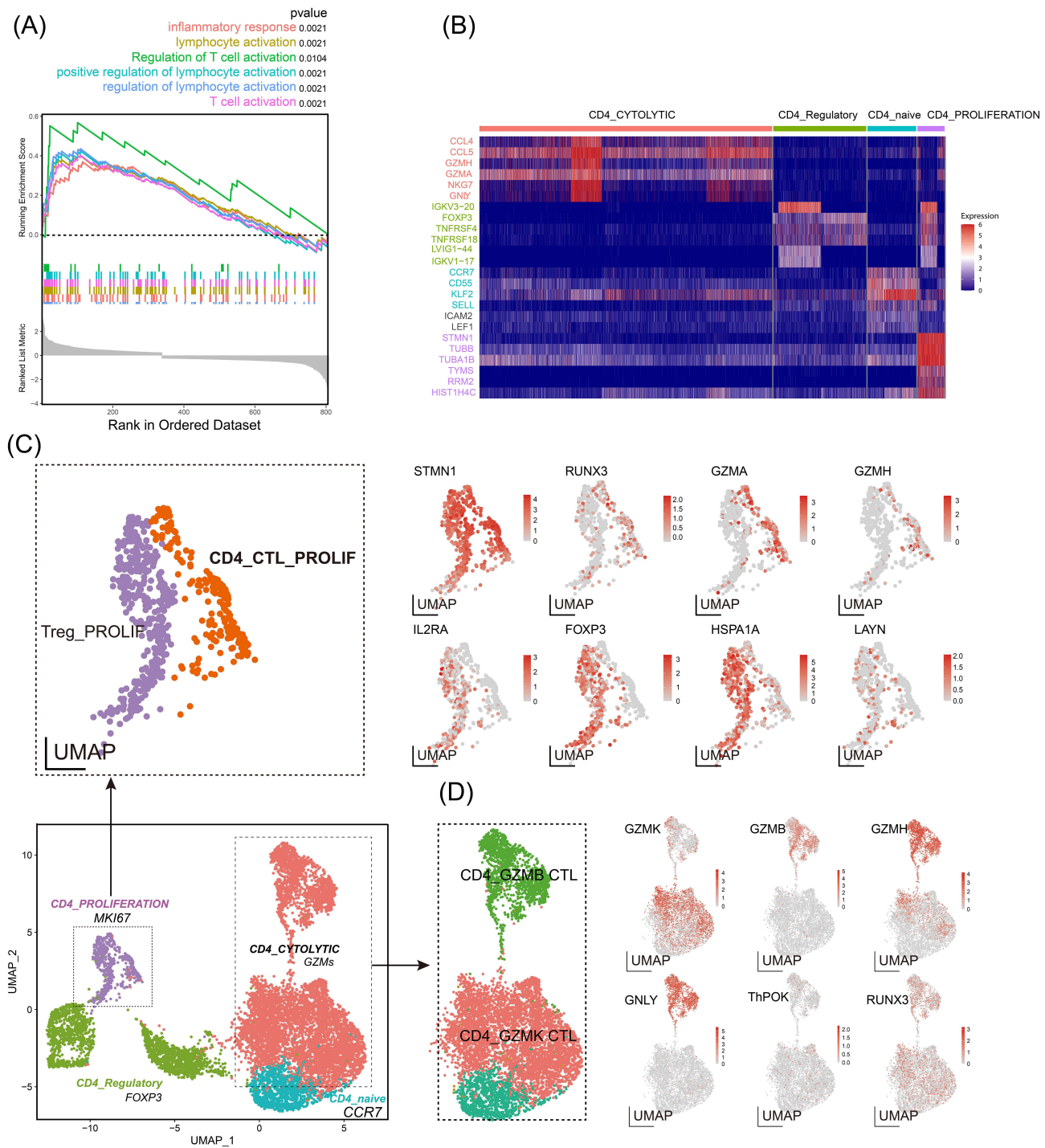


**Figure 2** Renal cell carcinoma exhibits heterogeneous proliferation and cytotoxic CD4<sup>+</sup> T cell states. **(A)** Gene set enrichment analysis revealed that the CD4\_CYTOTOXIC cluster was significantly enriched in immune activation pathways; **(B)** A higher-resolution clustering analysis further elucidated the heterogeneous nature of renal cell carcinoma, demonstrating diverse proliferation, regulatory, and cytotoxic CD4<sup>+</sup> T cell states; **(C)** Notably, the CD4\_PROLIFERATION cluster comprised distinct cell groups that co-expressed either cytotoxic or regulatory genes, but not both simultaneously; **(D)** Within the CD4\_CYTOTOXIC cluster, two distinct cytotoxic states were identified: CD4\_GZMK CTLs and CD4\_GZMB CTLs. These findings were visualized using the Uniform Manifold Approximation and Projection (UMAP) method, where each dot represents a single cell and is colored according to its respective cluster. CTLs refer to Cytotoxic CD4<sup>+</sup> T Cells.

## Renal Cell Carcinoma Possessed Heterogeneous Regulatory and Cytotoxic CD4<sup>+</sup> T Cell States

A high-resolution clustering analysis, focusing on a panel of feature genes encompassing CCL4, CCL5, GZMH, GZMA, NKG7, GNLY, IGKV3-20, FOXP3, TNFRSF4, TNFRSF18, IGLV1-44, IGKV1-17, CCR7, CD55, KLF2, SELL,



ICAM2, LEF1, STMN1, TUBB, TYMS, and RRM2, has unveiled the intricate heterogeneity of proliferative, regulatory, and cytotoxic CD4<sup>+</sup> T cell states within RCC (Figure 2B). Our findings reveal two distinct states of CD4\_CYTOTOXIC cells, with one subpopulation exhibiting a pronounced expression of cytotoxic lineage genes, including GZMH, NKG7, and GNLY. Furthermore, alongside these CD4\_CYTOTOXIC states, we identified a subgroup of regulatory CD4<sup>+</sup> T cells that exhibit a high level of immunoglobulin molecules, specifically IGKV3-20, IGLV1-44, and IGKV1-17 (Figure 2B). Intriguingly, the CD4\_PROLIFERATION cluster comprises distinct cell groups that exhibit a mutually exclusive expression pattern of either cytotoxic or regulatory genes, without a concurrent expression of both (Figure 2B).

To delve deeper into the cellular heterogeneity among CD4<sup>+</sup> T cells in RCC tissues, we implemented iterative re-clustering using cells originating from these four distinct clusters. In alignment with the findings from our high-resolution clustering analysis, we discovered two distinct states of CD4\_PROLIFERATION cells. Specifically, one subpopulation selectively exhibited high expression of GZMA, identified as CD4\_CTL\_PROLIF (cytotoxic CD4<sup>+</sup> proliferation cell, N = 149), while another subpopulation co-expressed high levels of FOXP3, designated as Treg\_PROLIF (Regulatory CD4<sup>+</sup> proliferation cell, N = 446) (Figure 2C). These Results suggest a distinct separation of CD4\_CYTOTOXIC and CD4\_Regulatory cells from CD4\_PROLIFERATION cells within the RCC milieu. Moreover, our re-clustering analysis revealed further refinement, classifying CD4\_Regulatory cells into Treg\_HSPA1A (N = 938) and Treg\_LAYN (N = 1098) states (Supplementary Figure 1A). The UMAP visualization highlighted that Treg\_HSPA1A cells exhibited a high co-expression of HSPA1A (Heat Shock Protein Family A (Hsp70) Member 1A), FOXP3, and immunoglobulin-related molecules. Conversely, Treg\_LAYN cells displayed a robust co-expression of FOXP3, TIGIT, and LAYN (Layilin) (Supplementary Figure 1B). Concurrently, our analysis identified two distinct cytotoxic cell states within the CD4\_CYTOTOXIC cluster: CD4\_GZMK (N = 4780) and CD4\_GZMB (N = 1627). Notably, CD4\_GZMK cells exhibited a high co-expression of GZMK and RUNX3 (Runt-Related Transcription Factor 3), which facilitates cytotoxic T cell differentiation. Conversely, the CD4\_GZMB state was characterized by a robust co-expression of GZMB, GZMH, GNLY, and RUNX3 (Figure 2D). Consistent with expectations, the CD4\_GZMK and CD4\_GZMB clusters did not express ThPOK (T-Helper-Inducing POZ/Krueppel-Like Factor), a crucial regulator of lineage commitment in immature T-cell precursors (Figure 2D).

To further validate the CD4\_GZMK and CD4\_GZMB T cell phenotype in tissues, multiplex immunofluorescence tissue staining of renal clear cell carcinoma samples revealed CD4<sup>+</sup> T cells co-expressing GZMB or GZMK (Figure 3A–E).

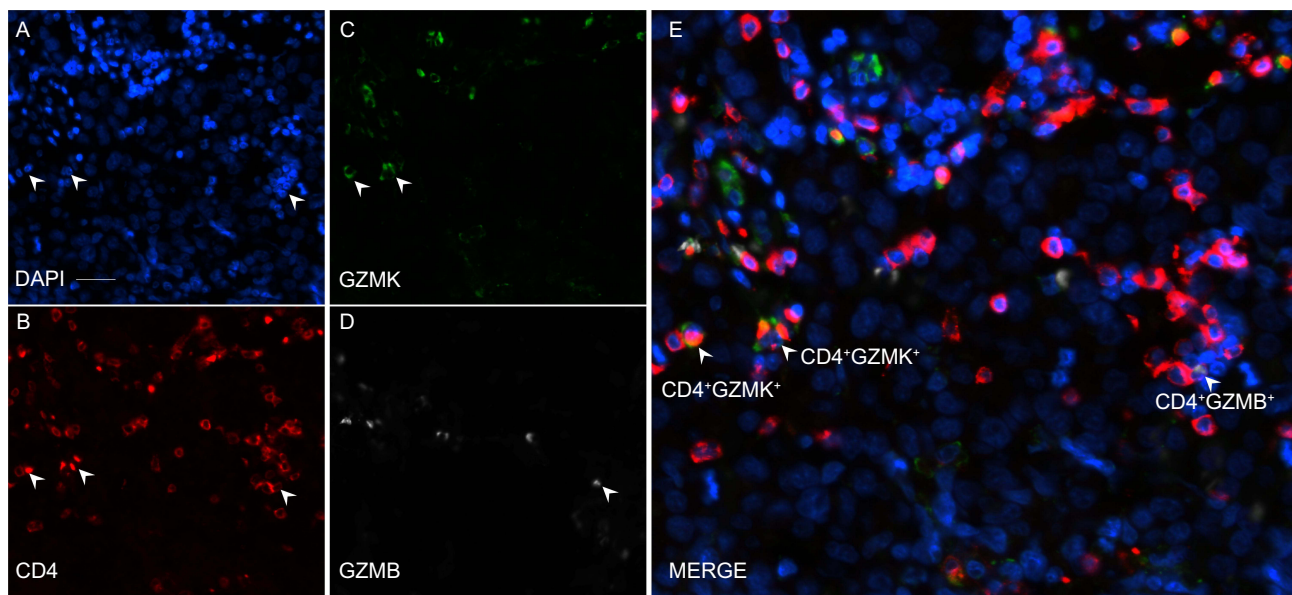


**Figure 3** Multiplex immunofluorescent staining was performed to visualize CD4<sup>+</sup>GZMK<sup>+</sup> and CD4<sup>+</sup>GZMB<sup>+</sup> cytotoxic T cells in renal clear cell carcinoma tissues. (A) Nuclei were labeled with DAPI (blue). (B) CD4 expression was marked in red. (C) GZMK expression was indicated by green fluorescence. (D) GZMB expression was labeled in white. (E) The merged image shows the co-localization of DAPI, CD4, GZMK, and GZMB signals. CD4<sup>+</sup> cells that concurrently expressed GZMK or GZMB were highlighted by arrowheads. Scale bar represents 200  $\mu$ m.



Intriguingly, both the CD4\_GZMK and CD4\_GZMB cell clusters displayed heightened activity (CD69<sup>+</sup>) and co-stimulation activation potential compared to the CD4\_Regulatory cluster within the RCC environment (Figure 4A and B). Moreover, we observed that CD4\_GZMB cells exhibited higher expression of cytotoxic lineage genes such as GZMB, GNLY, PRF1, TBX1, and NKG7,

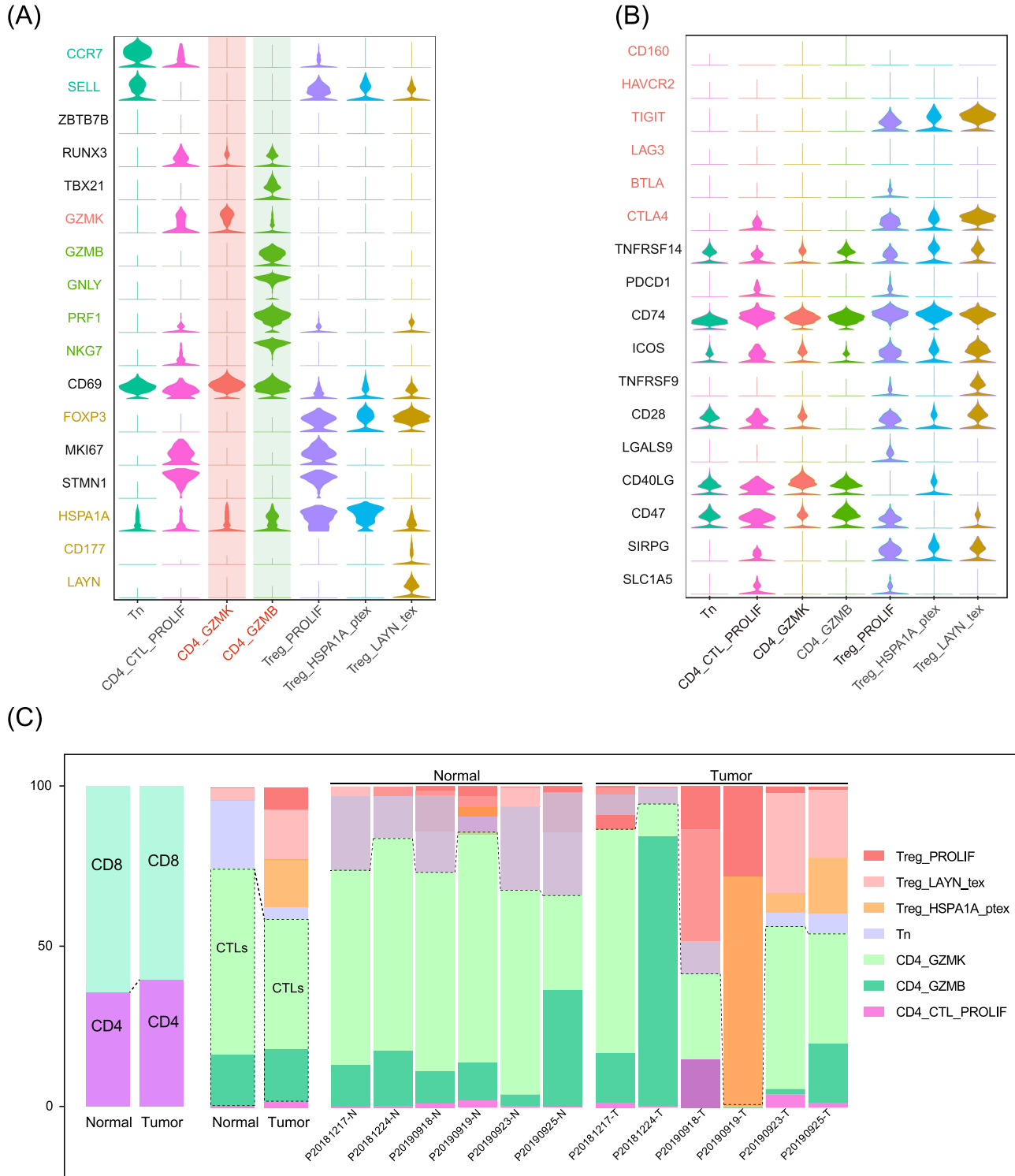


**Figure 4** The expression profile and phenotypic traits of cytotoxic CD4<sup>+</sup> T cells in renal cell carcinoma (RCC). **(A)** CD4\_GZMB cytotoxic T cells (CTLs) exhibited a heightened expression of cytotoxic lineage genes, such as GZMB, GNLY, PRF1, TBX1, and NKG7, in RCC samples; **(B)** In contrast, CD4\_Regulatory cells displayed a greater abundance of regulatory lineage genes, including CTLA4 and TIGIT; **(C)** The proportion of CD4<sup>+</sup> CTLs within RCC samples was evaluated, encompassing CD4\_GZMK CTLs, CD4\_GZMB CTLs, CD4\_CTL\_PROLIF, Tn, Treg\_PROLIF, Treg\_LAYN\_tex, and Treg\_HSPA1A\_ptex. CTLs refer to Cytotoxic CD4<sup>+</sup> T Cells.

and NKG7, suggesting a more robust cytotoxic or killing effect compared to CD4<sub>-</sub>GZMK cells in RCC samples (Figure 4A). Notably, each cluster comprised cells from diverse RCC patients, indicating that the expression states and clusters are conserved across individuals and not representative of patient-specific subpopulations, albeit with variations in their relative proportions (Figure 4C).

## CD4<sub>-</sub>GZMB Cluster Showed Stronger Cytotoxicity Than CD4<sub>-</sub>GZMK in RCC Environment

Heatmap analysis revealed an enrichment of multiple active cytotoxic CD4<sup>+</sup> T cell states, including CD4<sub>-</sub>GZMK, CD4<sub>-</sub>GZMB, and CD4<sub>-</sub>CTL\_PROLIF, in RCC samples. Notably, CD4<sub>-</sub>GZMK cells comprised the highest proportion (81%) among these cytotoxic states (Figure 5A). To directly assess the presence of CD4<sup>+</sup>GZMK<sup>positive</sup>GZMB<sup>negative</sup> and CD4<sup>+</sup>GZMB<sup>positive</sup>GZMK<sup>negative</sup> cells in RCC in situ, multiplex immunofluorescent staining for CD4, GZMK, and GZMB was performed on renal tumor sections from 20 patients. Our analysis revealed that CD4<sup>+</sup>GZMK<sup>positive</sup>GZMB<sup>negative</sup> cells were detected in 14 out of 20 cases, while CD4<sup>+</sup>GZMB<sup>positive</sup>GZMK<sup>negative</sup> cells were identified in 6 of the 20 RCC cases. Notably, both CD4<sup>+</sup>GZMK<sup>positive</sup>GZMB<sup>negative</sup> and CD4<sup>+</sup>GZMB<sup>positive</sup>GZMK<sup>negative</sup> cells were concurrently observed in 5 RCC patients (Figure 3A–E). To delve deeper into the functional disparities between the CD4<sub>-</sub>GZMB and CD4<sub>-</sub>GZMK cell clusters, we performed GSEA to identify altered pathways between these two clusters. Our analysis revealed that the CD4<sub>-</sub>GZMB cell cluster was enriched in cytotoxic-related pathways, including cell killing, leukocyte-mediated cytotoxicity, T cell activation, T cell-mediated cytotoxicity, and tumor necrosis factor production (Figure 5B). Furthermore, we derived immune-related scores (IRs) for single cells to dissect the functional characteristics of each cell subpopulation. As depicted in the figure (Figure 5C), the CD4<sub>-</sub>Regulatory cluster, comprising Treg\_HSPA1A and Treg\_LAYN, exhibited higher IRs related to T\_CELL\_TOLERANCE and T\_CELL\_HOMEOSTASIS. Conversely, the CD4<sub>-</sub>GZMB cluster displayed higher AUC scores associated with T\_CELL\_MEDIATED\_CYTOTOXICITY and GO\_BP\_CYTOLYSIS.

## Both Regulatory T Cells and CD4<sup>+</sup> CTLs are Derives from Proliferating CD4<sup>+</sup> T Cells in RCC Tissues

Utilizing CytoTRACE analysis, we investigated the differentiation or stemness status of CD4<sup>+</sup> T cell subpopulations within a single-cell RNA sequencing dataset. Our calculations revealed that CD4<sub>-</sub>PROLIFERATION cells, comprising Treg\_PROLIF and CD4<sub>-</sub>CTL\_PROLIF, displayed the highest stemness scores and the lowest differentiation status. Conversely, CD4<sup>+</sup>GZMK<sup>positive</sup>GZMB<sup>negative</sup> and Treg\_LAYN cells exhibited the lowest stemness scores and the highest differentiation states within RCC tissues (Figure 6A). Analysis revealed that housekeeping genes, including GAPDH (Glyceraldehyde-3-Phosphate Dehydrogenase), ACTB (Actin Beta), and ACTG1 (Actin Gamma 1), were specifically associated with a less differentiated state of CD4<sup>+</sup> T cells. Conversely, cytotoxic-linked genes such as GZMK, TNF-related activation protein TNFSF5 (Tumor Necrosis Factor Superfamily, Member 5, or CD40L), and the transcription factor FOS (Fos Proto-Oncogene, AP-1 Transcription Factor Subunit), were found to be associated with a higher differentiated state of CD4<sup>+</sup> T cells (Figure 6B). Furthermore, pseudotime trajectory analysis distinguished CD4<sub>-</sub>PROLIFERATION cells into two distinct groups: Treg\_PROLIF (CD4<sup>+</sup>STMN1<sup>+</sup>FOXP3<sup>+</sup>) and CD4<sub>-</sub>CTL\_PROLIF (CD4<sup>+</sup>STMN1<sup>+</sup>GZMK<sup>+</sup>). Notably, each group of cells aligned along a unique branch, representing proliferating cytotoxic or regulatory CD4<sup>+</sup> T lymphocytes within the mRCC microenvironment (Figure 6C and Supplementary Figure 2A–C).

Hierarchical clustering analysis, utilizing genes related to CD4<sub>-</sub>PROLIFERATION, CD4<sub>-</sub>Regulatory, and CD4<sub>-</sub>CYTOTOXIC functions, revealed a striking resemblance in the expression patterns of CD4<sub>-</sub>PROLIFERATION and CD4<sub>-</sub>Regulatory cells (Figure 6D). Moreover, when compared to CD4<sup>+</sup>GZMK<sup>positive</sup>GZMB<sup>negative</sup> cells, the expression patterns of CD4<sup>+</sup>GZMB<sup>positive</sup>GZMK<sup>negative</sup> and CD4<sub>-</sub>PROLIFERATION cells exhibited a higher degree of consistency (Figure 6D). These preliminary analyses hinted at the potential derivation of weakly cytotoxic CD4<sup>+</sup>GZMK<sup>positive</sup>GZMB<sup>negative</sup> cells from their more cytotoxic CD4<sup>+</sup>GZMB<sup>positive</sup>GZMK<sup>negative</sup> counterparts within RCC tissues.

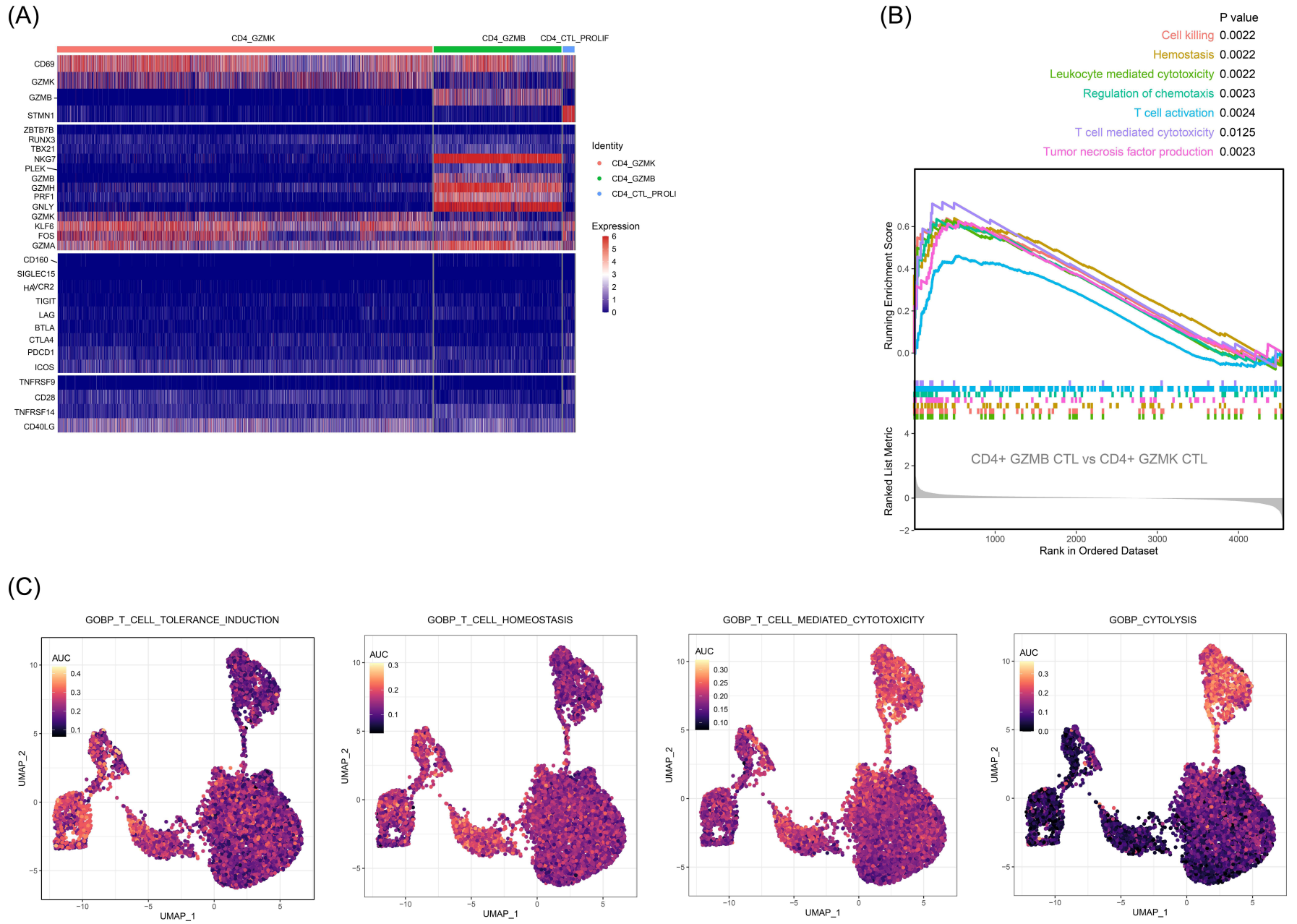


**Figure 5** The CD4\_GZMB CTLs cluster exhibited greater cytotoxicity than CD4\_GZMK in the renal cell carcinoma (RCC) microenvironment. **(A)** High-resolution clustering analysis revealed that multiple active cytotoxic CD4<sup>+</sup> T cell states, including CD4\_GZMK, CD4\_GZMB, and CD4\_CTL\_PROLIF were enriched in RCC samples; **(B)** Gene set enrichment analysis demonstrated that the CD4\_GZMB cluster was significantly enriched in pathways related to cytotoxicity; **(C)** Notably, the CD4\_GZMB cluster showed higher AUC scores associated with T\_CELL\_MEDIATED\_CYTOTOXICITY and GO\_BP\_CYTOLYSIS, indicating a stronger cytotoxic potential.

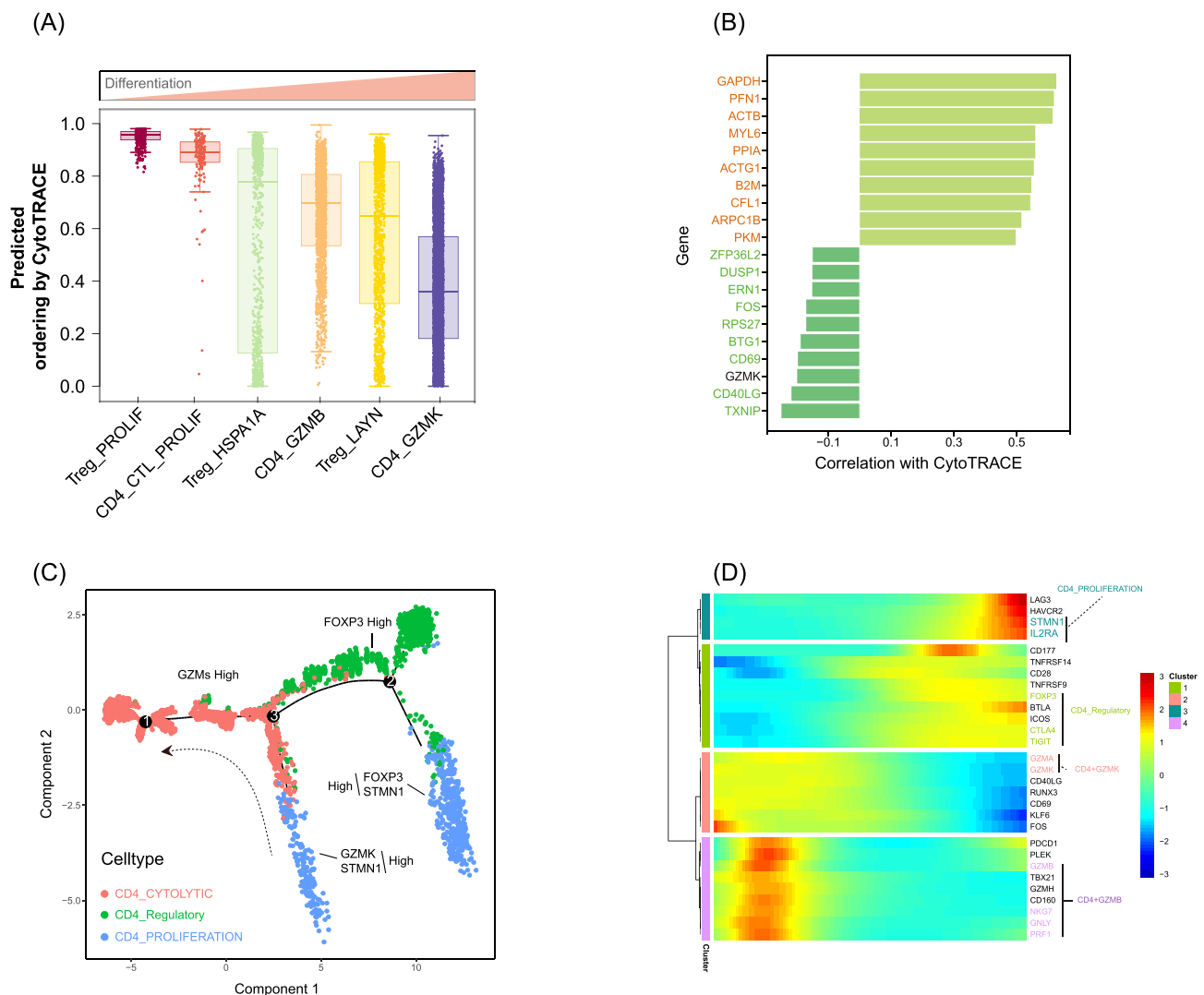


**Figure 6** Both Regulatory T Cells And CD4<sup>+</sup> CTLs Are Derives From Proliferating CD4<sup>+</sup> T Cells In RCC Tissues. **(A)** According to CytoTRACE analysis, CD4\_PROLIFERATION cells, comprising Treg\_PROLIF and CD4\_CTL\_PROLIF, exhibited notably high stemness scores and a minimal degree of differentiation. Conversely, CD4\_GZMK CTLs and Treg\_LAYN displayed the lowest stemness scores and a pronounced level of differentiation in RCC tissues; **(B)** The cytotoxic linkage genes GZMK, TNFSF5, and the transcription factor FOS were found to correlate with a more differentiated state in CD4<sup>+</sup> T cells; **(C)** Pseudotime trajectory analysis revealed that CD4\_PROLIFERATION cells segregated into Treg\_PROLIF and CD4\_CTL\_PROLIF groups, with each group aligning along distinct branches representing proliferating cytotoxic or regulatory CD4<sup>+</sup> T lymphocytes; **(D)** Hierarchical clustering analysis highlighted the striking similarity in expression patterns between CD4\_PROLIFERATION and CD4\_Regulatory cells. Furthermore, when compared to CD4\_GZMK CTLs, the expression patterns of CD4\_GZMB CTLs and CD4\_PROLIFERATION displayed a more consistent alignment.

## Cytotoxic CD4<sup>+</sup> T Cells Predicts Clinical Response to Immune Checkpoint Inhibitors

To delve deeper into the association between cytotoxic CD4<sup>+</sup> T lymphocytes and immunotherapy, we analyzed the EGAD00001008166 dataset encompassing two RCC patients—a responder and a non-responder, following immunotherapy with ICIs (Figure 7A). Notably, CD8<sup>+</sup> T cells continued to constitute a larger proportion compared to CD4<sup>+</sup> T cells in both RCC samples treated with ICIs (Figure 7B). UMAP analysis highlighted differences in the distribution of CD4<sup>+</sup> T cells between ICIs responders and non-responders. Specifically, CD4<sup>+</sup> T cells from responder patients were predominantly located towards the inner region of the scatter plot, while those from non-responder patients were more prominent in the outer region (Figure 7C). Intriguingly, CD4<sup>+</sup> T cells in responder patients exhibited high expression levels of cytotoxic-linked genes and transcription factors, such as GZMK and NR4A2. Conversely, CD4<sup>+</sup> T cells from non-responder patients co-expressed high levels of regulatory and inhibitory molecules, including FOXP3 and CTLA4 (Cytotoxic T-Lymphocyte-Associated Protein 4) (Figure 7C). Analogous to CD4<sup>+</sup> T cells, CD8<sup>+</sup> T cells in the ICIs

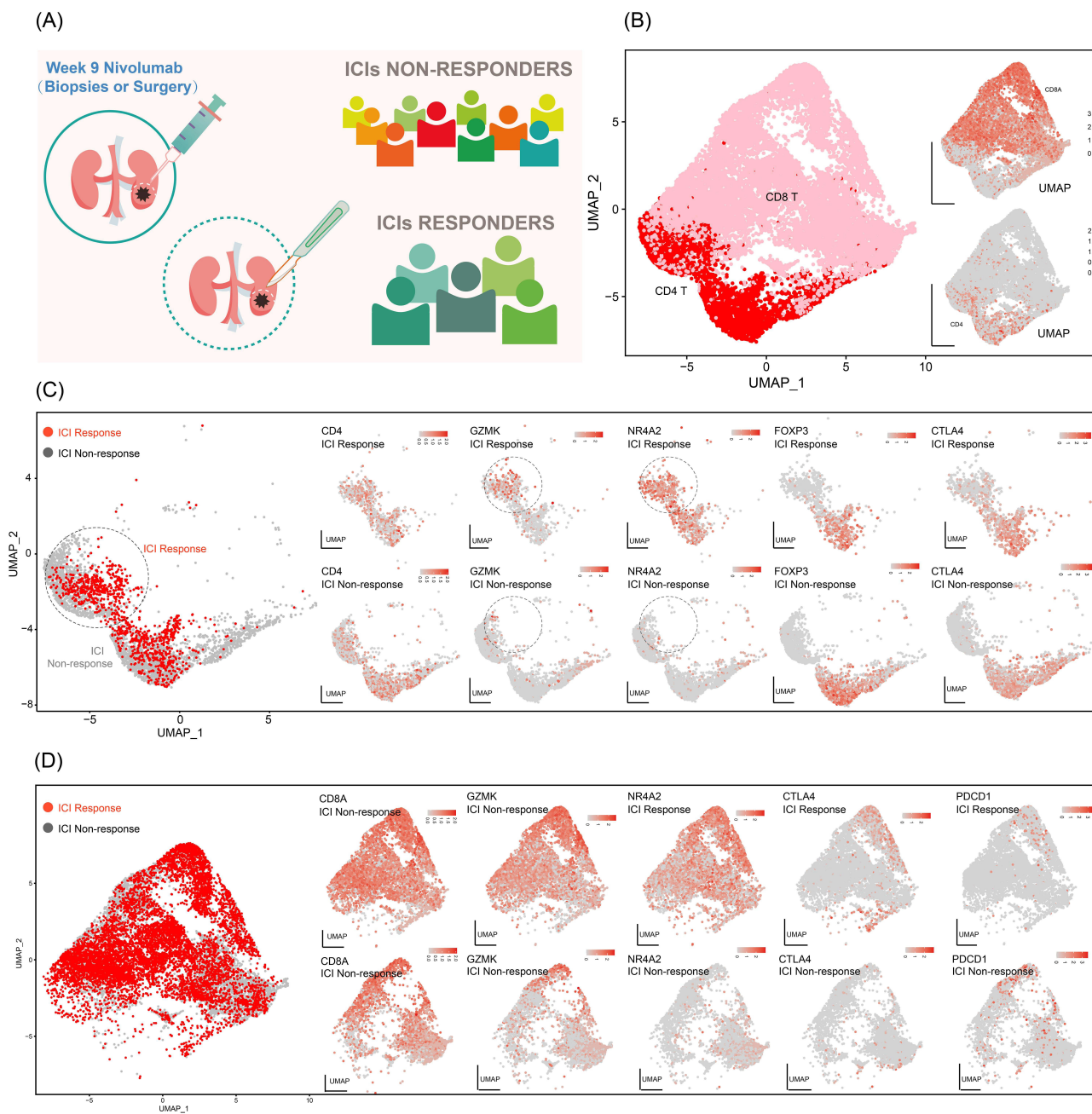


**Figure 7** Cytotoxic CD4+ T Cells Predicts Clinical Response To Immune Checkpoint Inhibitors. **(A)** Two distinct renal cell carcinoma patients were analyzed post-treatment with immune checkpoint inhibitors (9 weeks of Nivolumab), one demonstrating a responder status and the other a non-responder status; **(B)** A uniform manifold approximation and projection (UMAP) analysis revealed that CD8+ T cells accounted for a larger percentage compared to CD4+ T cells in both renal cell carcinoma patients; **(C)** The UMAP analysis further delineated the distribution of CD4+ T cells between the responder and non-responder patients following immune checkpoint inhibitor (ICI) treatment. CD4+ T cells from responder patients exhibited elevated expression levels of cytotoxic linkage genes and transcription factors, including GZMK and NR4A2. Conversely, CD4+ T cells from non-responder patients co-expressed high levels of regulatory and inhibitory linkage molecules, such as FOXP3 and CTLA4; **(D)** Among CD8+ T cells, those from responder patients displayed higher expression levels of GZMK and NR4A2. In contrast, non-responder patients exhibited a higher percentage of cells expressing PDCD1/PD1.

responder group displayed higher expression of GZMK and NR4A2, while non-responder patients exhibited a higher percentage of PDCD1/PD1 (Programmed Cell Death 1) (Figure 7D).

Subsequently, we evaluated the predictive capacity of CD4+ CTLs for immunotherapy response using bulk RNA-seq or microarray data from the Checkmate 009, Checkmate 010, and Checkmate 025 cohorts. Our findings revealed that post-ICI RCC patients exhibited a significantly higher proportion of CD4+ CTLs compared to the pre-ICI group ( $P =$



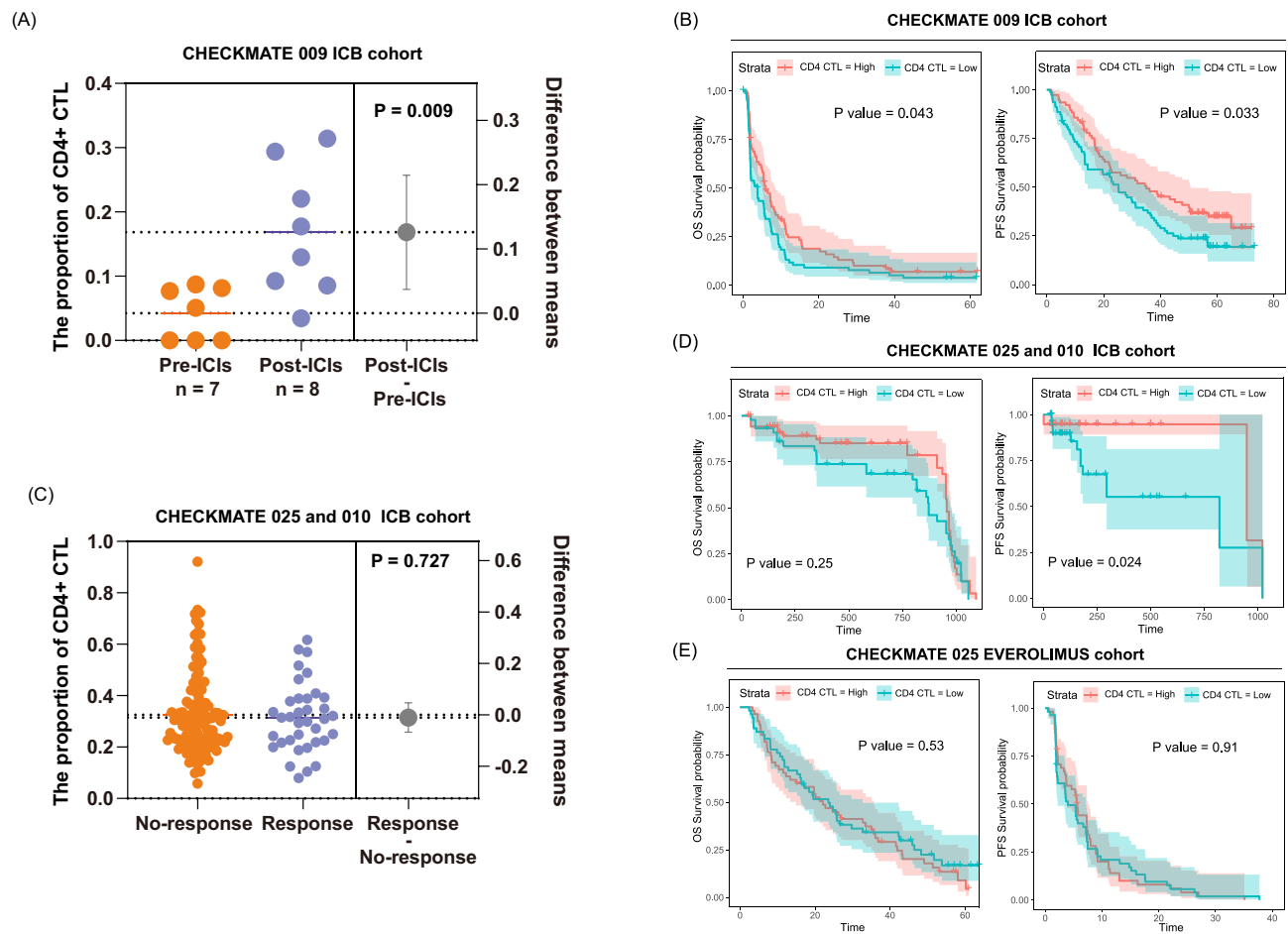


**Figure 8** Cytotoxic CD4+ T Cells (CD4+ CTLs) improve Clinical Response To Immune Checkpoint Inhibitors. **(A)** Renal cell carcinoma (RCC) patients treated with immune checkpoint inhibitors (ICIs) exhibited an increased proportion of CD4+ cytotoxic T lymphocytes; **(B)** Analysis of the Checkmate 009 ICIs cohort revealed that patients with a higher proportion of CD4+ CTLs achieved improved overall survival and progression-free survival probabilities. **(C)** However, in the Checkmate 010 and Checkmate 025 cohorts, no significant difference in the proportion of CD4+ CTLs was observed between ICIs responders and non-responders; **(D)** Interestingly, a higher proportion of CD4+ CTLs in clear cell renal cell carcinoma (ccRCC) patients from the Checkmate 010 and Checkmate 025 ICIs cohorts was associated with a decreased progression-free survival probability; **(E)** The Checkmate 025 everolimus cohort demonstrated that the expression of CD4+ CTLs was not correlated with overall survival or progression-free survival probabilities.

0.009) (Figure 8A). Notably, patients with a higher proportion of CD4+ CTLs displayed improved overall survival ( $P = 0.043$ ) and progression-free survival ( $P = 0.033$ ) (Figure 8B). However, when analyzing the Checkmate 010 and Checkmate 025 cohorts, we observed no significant difference in the proportion of CD4+ CTLs between ICI responders and non-responders (Figure 8C). Interestingly, in the Checkmate 025 cohort specifically, a higher proportion of CD4+ CTLs was associated with decreased progression-free survival among ccRCC patients ( $P = 0.024$ ) (Figure 8D). Conversely, the expression levels of CD4+ CTLs did not correlate with overall survival ( $P = 0.53$ ) or progression-free survival ( $P = 0.91$ ) in the Checkmate 025 everolimus cohort (Figure 8E).

## Discussion

As the reality dawns that only a fraction of solid cancer patients respond favorably to checkpoint inhibitor therapy, and some cancer types exhibit no response at all, a deeper understanding of the functional regulation and precise mechanisms of cytotoxic CD4<sup>+</sup> T lymphocytes becomes paramount. This knowledge may pave the way for more efficacious and groundbreaking immunotherapies that target this effector population, either independently or in tandem with traditional CD8<sup>+</sup> T lymphocytes. In our current study, we have pioneered the identification of the prevalent presence of fully functional cytotoxic CD4<sup>+</sup> T lymphocyte subtypes and elucidated their associations with immunotherapy response in renal cell carcinoma patients. Our analysis of tumor-infiltrating CD4<sup>+</sup> T cells based on scRNA-seq data aligns with

previous research, confirming that tumor-specific CD4<sup>+</sup> T cells encompass four major cell states.<sup>19</sup> This convergence in findings strengthens the body of evidence regarding the diversity and complexity of CD4<sup>+</sup> T cell responses in the tumor microenvironment. A direct ex vivo analysis of sorted cancer-specific CD4<sup>+</sup> T cells confirmed the presence of cytotoxic-associated genes in samples from both peripheral blood and tumor-infiltrating lymphocytes or lymph nodes (TILs/TILNs). Furthermore, the cytotoxic CD4<sup>+</sup> T cell subsets identified in bladder tumors, non-small cell lung carcinoma, melanoma, and hepatocellular carcinoma exhibited clonal expansion, suggesting their emergence as a consequence of recognition of cognate tumor antigens.<sup>19,32,33</sup> Extensive ex vivo investigations have unequivocally established that these tumor-specific CD4<sup>+</sup> CTLs play a pivotal role in anti-tumor immunity, achieving tumor cell elimination through contact-dependent mechanisms.<sup>34</sup> Single-cell cytotoxicity assays conducted on CD4<sup>+</sup> CTLs, specifically targeting tumor antigens such as MAGE-A3 and NY-ESO-1, isolated using MHC class II tetramers, have unequivocally demonstrated their ability to directly eliminate autologous tumor cells. This killing efficiency was further augmented when tumor cells were pre-treated with interferon gamma (IFN- $\gamma$ ) or stably transduced with the class II major histocompatibility complex transactivator (CIITA) to enhance MHC class II gene expression.<sup>19</sup> This killing mechanism was directly reliant on the activity of perforin and granzyme. Additionally, incubation with an agonistic antibody targeting the SLAM Family Member 7 (SLAMF7) activating co-receptor partially potentiated the cytotoxic effect of CD4<sup>+</sup> T cells in melanoma.<sup>19</sup> The direct killing effect and associated molecular mechanisms of cytotoxic CD4<sup>+</sup> T cells have also been validated in bladder cancer.<sup>22</sup> We similarly observed that CD4<sup>+</sup> CTLs in RCC samples expressed high levels of perforin and granzyme molecules, including GZMA, GZMK, GZMB, GZMH, and PRF1.

Our scRNA-seq data analysis revealed that cytotoxic CD4<sup>+</sup> T cells constitute the largest subset of CD4<sup>+</sup> T cells in both cancerous and adjacent para-cancerous tissues of RCC patients. Interestingly, we noted that, in comparison to para-cancerous tissue, cancerous tissue contained a lower proportion of CD4<sup>+</sup> CTLs and a higher proportion of regulatory CD4<sup>+</sup> T cells in RCC patients. On the other hand, CD4<sup>+</sup> T cells from patients responding to ICIs exhibited high expression levels of cytotoxic-associated genes and transcription factors, such as GZMK and NR4A2. Conversely, CD4<sup>+</sup> T cells from non-responder patients co-expressed high levels of regulatory and inhibitory molecules, including FOXP3 and CTLA4. Furthermore, post ICIs treatment RCC samples displayed a more pronounced CD4<sup>+</sup> CTL signature. These findings suggest that a shift in the CD4<sup>+</sup> CTLs/Tregs balance, favoring regulatory CD4<sup>+</sup> T cells, may play a pivotal role in immune tolerance and escape mechanisms. It is noteworthy that previous studies have reported that the relative balance between the activation of CD4<sup>+</sup> CTLs and inhibitory regulatory CD4<sup>+</sup> T cells plays a crucial role in promoting the killing of autologous tumors in bladder cancer.<sup>22</sup> Furthermore, the expansion of regulatory CD4<sup>+</sup> T cells can inhibit the activity of CD4<sup>+</sup> CTLs through cell-cell interactions and the release of cytokines in the tumor microenvironment. Integrating our analysis with previous studies, we postulate that cytotoxic CD4<sup>+</sup> T cells also contribute a direct anti-tumor immune response in RCC patients. Notably, the transcription factor T-BET, which is well-known for inducing the expression of GZMB and perforin essential for cytotoxic CD8<sup>+</sup> T cell function, may play a similar role in CD4<sup>+</sup> CTLs.<sup>35</sup> In the context of an acute influenza virus infection model, the expression of T-BET is predominantly observed at the effector sites, where it plays a pivotal role in fostering the differentiation of cytotoxic CD4<sup>+</sup> T cells.<sup>36</sup> Indeed, during thymic development, the ThPOK transcription factor plays a definitive role in specifying the lineage commitment of CD4<sup>+</sup> lymphocytes. Furthermore, for CD4<sup>+</sup> CTLs residing within intraepithelial lymphocytes, the generation of cytotoxic CD4<sup>+</sup> T cell subsets necessitates both the loss of ThPOK expression and the coordinated signaling from the RUNX3 and TBET-TBX21 axis.<sup>37,38</sup> In our current study, we have observed that CD4<sup>+</sup> CTLs express a high level of RUNX3 and a low level of ThPOK, indicating that the tumor microenvironment in RCC tissues fosters tolerance by suppressing CD4<sup>+</sup> CTLs and their related transcription factor expression.

A comprehensive series of studies exploring the differentiation of CD4<sup>+</sup> T lymphocytes into CD4<sup>+</sup> CTLs has illuminated their cellular origins. These investigations lend support to the notion that CD4<sup>+</sup> CTLs can arise from various helper T cell effector subsets, encompassing Th0, Th1, Th2, Th17, and Tregs.<sup>39–42</sup> In this study, our analysis revealed that both CD4<sup>+</sup> CTLs and regulatory T cells originate from a distinct subset of CD4<sup>+</sup> T cells, designated as the CD4\_PROLIFERATION cell cluster. This cluster expresses high levels of proliferation-associated genes such as ZWINT, MKI67, PCNA, and TYMS, based on CytoTRACE, pseudotime trajectory, and hierarchical clustering analyses. Furthermore, CytoTRACE analysis indicated that CD4<sup>+</sup>GZMK<sup>positive</sup>GZMB<sup>negative</sup> cells and Treg\_LAYN cells exhibited

the lowest stemness scores and attained the highest levels of differentiation, suggesting that CD4<sup>+</sup>GZMK<sup>positive</sup>GZMB<sup>negative</sup> cells undergo differentiation from CD4<sup>+</sup>GZMB<sup>positive</sup>GZMK<sup>negative</sup> cells within the RCC environment. This finding aligns with previous reports by David Y. Oh et al, who documented the presence of proliferative CD4<sup>+</sup> T cells encompassing CD4<sup>+</sup> CTL and regulatory T cell states in bladder cancer.<sup>22</sup> Intriguingly, our findings reveal that CD4<sup>+</sup>GZMB<sup>positive</sup>GZMK<sup>negative</sup> cells exhibit greater cytotoxicity than CD4<sup>+</sup>GZMK<sup>positive</sup>GZMB<sup>negative</sup> cells within the RCC microenvironment. Notably, the proportion of weakly cytotoxic CD4<sup>+</sup>GZMK<sup>positive</sup>GZMB<sup>negative</sup> cells is significant, and immunotherapy with ICIs increases the number of highly cytotoxic CD4<sup>+</sup>GZMB<sup>positive</sup>GZMK<sup>negative</sup> cells in the RCC milieu. These results imply that the cancer environment compromises the anti-tumor immunity of CD4<sup>+</sup> CTLs in two distinct ways: first, by inhibiting the differentiation of proliferative CD4<sup>+</sup> T cells into cytotoxic CD4<sup>+</sup> T cells; and second, by fostering the differentiation of highly cytotoxic CD4<sup>+</sup>GZMB<sup>positive</sup>GZMK<sup>negative</sup> cells into weakly cytotoxic CD4<sup>+</sup>GZMK<sup>positive</sup>GZMB<sup>negative</sup> cells. Moreover, previous research has demonstrated that the cytotoxic potential of CD4<sup>+</sup> CTLs against cancer cells can be hampered by regulatory T cells. Notably, the elimination of Tregs has been shown to augment tumor eradication mediated by CD4<sup>+</sup> CTLs.<sup>22</sup>

We acknowledge that this study has several limitations. Firstly, the retrospective design and potential selection bias are notable drawbacks, and the lack of our own immunotherapy cohort and single-cell sequencing data targeting CD4<sup>+</sup> T lymphocytes from our center is a limitation. Additionally, the reliance on single-cell RNA sequencing data from a limited number of patients may not fully capture the heterogeneity of mRCC. Secondly, the validation using multiple immunofluorescence in only a small number of cases is relatively superficial. In future studies, more robust methods such as flow cytometry or mass cytometry (CyTOF) should be employed for verification. Finally, the work presented in this study is purely correlative and does not provide any mechanistic explanations. The regulatory mechanism underlying the differentiation of CD4<sup>+</sup> CTLs and their role in enhancing ICIs response in RCC remains to be further investigated.

## Conclusion

In summary, our study lays an essential conceptual groundwork for advancing immunotherapy in mRCC. Notably, we discovered that cytotoxic CD4<sup>+</sup> T cells constitute a significant proportion among all CD4<sup>+</sup> T lymphocyte sub-clusters in RCC patients. Moreover, we were able to further discern two distinct cytotoxic states within these cells: CD4<sup>+</sup>GZMK<sup>positive</sup> T cells exhibiting weak cytotoxicity and CD4<sup>+</sup>GZMB<sup>positive</sup> T cells demonstrating robust cytotoxic activity. Our preliminary analysis suggests that these cells originate from CD4\_PROLIFERATION cells, and interestingly, weak cytotoxic CD4<sup>+</sup>GZMK<sup>positive</sup>GZMB<sup>negative</sup> cells may differentiate from highly cytotoxic CD4<sup>+</sup>GZMB<sup>positive</sup>GZMK<sup>negative</sup> cells within the RCC environment. Furthermore, our study highlights the distinct expression patterns of cytotoxic-associated molecules in CD4<sup>+</sup> CTLs and their potential synergistic role in enhancing ICIs response in mRCC patients. Collectively, our findings indicate that intratumoral CD4<sup>+</sup> CTLs play a pivotal role in anti-tumor immunity, presenting as a promising biomarker for predicting ICIs response in mRCC patients.

## Data Sharing Statement

The data generated are included in the manuscript and [Supplementary Data](#).

## Acknowledgment

This paper has been uploaded to ResearchGate as a preprint: <https://www.researchgate.net/publication/376296105>  
[Single-cell analysis identifies distinct populations of cytotoxic CD4 T cells CD4 CTLs linked to the therapeutic efficacy of immune checkpoint inhibitors in metastatic renal cell carcinoma](#)

## Author Contributions

All authors made a significant contribution to the work reported, whether that is in the conception, study design, execution, acquisition of data, analysis and interpretation, or in all these areas; took part in drafting, revising or critically reviewing the article; gave final approval of the version to be published; have agreed on the journal to which the article has been submitted; and agree to be accountable for all aspects of the work.

## Funding

This study was supported by the innovate Fund for scientific research, Fujian Medical University (Grant number:2021QNA012).

## Disclosure

The authors declare that they have no competing interests in this work.

## References

- Sung H, Ferlay J, Siegel RL, et al. Global cancer statistics 2020: GLOBOCAN estimates of incidence and mortality worldwide for 36 cancers in 185 countries. *Ca a Cancer J Clinicians*. 2021;71(3):209–249. doi:10.3322/caac.21660
- Capitanio U, Montorsi F. Renal cancer. *Lancet*. 2016;387(10021):894–906. doi:10.1016/S0140-6736(15)00046-X
- Choueiri TK, Longo DL, Motzer RJ. Systemic therapy for metastatic renal-cell carcinoma. *N Engl J Med*. 2017;376(4):354–366. doi:10.1056/NEJMra1601333
- Kim TK, Vandsemb EN, Herbst RS, Chen L. Adaptive immune resistance at the tumour site: mechanisms and therapeutic opportunities. *Nat Rev Drug Discov*. 2022;21(7):529–540. doi:10.1038/s41573-022-00493-5
- Motzer RJ, Escudier B, McDermott DF, et al. Nivolumab versus everolimus in advanced renal-cell carcinoma. *N Engl J Med*. 2015;373(19):1803–1813. doi:10.1056/NEJMoa1510665
- Hellmann MD, Paz-Ares L, Bernabe Caro R, et al. Nivolumab plus ipilimumab in advanced non–small-cell lung cancer. *N Engl J Med*. 2019;381(21):2020–2031. doi:10.1056/NEJMoa1910231
- Motzer RJ, Jonasch E, Michaelson MD, et al. NCCN guidelines insights: kidney cancer, version 2.2020. *J National Compr Cancer Network*. 2019;17(11):1278–1285. doi:10.6004/jnccn.2019.0054
- Motzer RJ, Tannir NM, McDermott DF, et al. Nivolumab plus Ipilimumab versus sunitinib in advanced renal-cell carcinoma. *N Engl J Med*. 2018;378(14):1277–1290. doi:10.1056/NEJMoa1712126
- Tumeh PC, Harview CL, Yearley JH, et al. PD-1 blockade induces responses by inhibiting adaptive immune resistance. *Nature*. 2014;515(7528):568–571. doi:10.1038/nature13954
- Herbst RS, Soria J-C, Kowanetz M, et al. Predictive correlates of response to the anti-PD-L1 antibody MPDL3280A in cancer patients. *Nature*. 2014;515(7528):563–567. doi:10.1038/nature14011
- Giraldo NA, Becht E, Pagès F, et al. Orchestration and prognostic significance of immune checkpoints in the microenvironment of primary and metastatic renal cell cancer. *Clin Cancer Res*. 2015;21(13):3031–3040. doi:10.1158/1078-0432.CCR-14-2926
- Au L, Hatipoglu E, Robert de Massy M, et al. Determinants of anti-PD-1 response and resistance in clear cell renal cell carcinoma. *Cancer Cell*. 2021;39(11):1497–1518.e1411. doi:10.1016/j.ccell.2021.10.001
- Rodig SJ, Gusenleitner D, Jackson DG, et al. MHC proteins confer differential sensitivity to CTLA-4 and PD-1 blockade in untreated metastatic melanoma. *Sci Transl Med*. 2018;10(450). doi:10.1126/scitranslmed.aar3342
- Hunder NN, Wallen H, Cao J, et al. Treatment of metastatic melanoma with autologous CD4+ T Cells against NY-ESO-1. *N Engl J Med*. 2008;358(25):2698–2703. doi:10.1056/NEJMoa0800251
- Tran E, Turcotte S, Gros A, et al. Cancer immunotherapy based on mutation-specific CD4+ T cells in a patient with epithelial cancer. *Science*. 2014;344(6184):641–645. doi:10.1126/science.1251102
- Linnemann C, van Buuren MM, Bies L, et al. High-throughput epitope discovery reveals frequent recognition of neo-antigens by CD4+ T cells in human melanoma. *Nature Med*. 2014;21(1):81–85. doi:10.1038/nm.3773
- Wing JB, Tanaka A, Sakaguchi S. Human FOXP3+ regulatory T cell heterogeneity and function in autoimmunity and cancer. *Immunity*. 2019;50(2):302–316. doi:10.1016/j.immuni.2019.01.020
- Wen YJ, Min R, Tricot G, Barlogie B, Yi Q. Tumor lysate-specific cytotoxic T lymphocytes in multiple myeloma: promising effector cells for immunotherapy. *Blood*. 2002;99(9):3280–3285. doi:10.1182/blood.V99.9.3280
- Cachot A, Bilous M, Liu YC, et al. Tumor-specific cytolytic CD4 T cells mediate immunity against human cancer. *Sci Adv*. 2021;7(9). doi:10.1126/sciadv.abe3348
- Porakishvili N, Kardava L, Jewell AP, et al. Cytotoxic CD4+ T cells in patients with B cell chronic lymphocytic leukemia kill via a perforin-mediated pathway. *Haematologica*. 2004;89(4):435–443.
- Kitano S, Tsuji T, Liu C, et al. Enhancement of tumor-reactive cytotoxic CD4+ T cell responses after ipilimumab treatment in four advanced melanoma patients. *Cancer Immunol Res*. 2013;1(4):235–244. doi:10.1158/2326-6066.CIR-13-0068
- Oh DY, Kwek SS, Raju SS, et al. Intratumoral CD4+ T cells mediate anti-tumor cytotoxicity in human bladder cancer. *Cell*. 2020;181(7):1612–1625.e1613. doi:10.1016/j.cell.2020.05.017
- Zheng L, Qin S, Si W, et al. Pan-cancer single-cell landscape of tumor-infiltrating T cells. *Science*. 2021;374:6574. doi:10.1126/science.abe6474
- Bi K, He MX, Bakouny Z, et al. Tumor and immune reprogramming during immunotherapy in advanced renal cell carcinoma. *Cancer Cell*. 2021;39(5):649–661.e645. doi:10.1016/j.ccell.2021.02.015
- Braun DA, Hou Y, Bakouny Z, et al. Interplay of somatic alterations and immune infiltration modulates response to PD-1 blockade in advanced clear cell renal cell carcinoma. *Nature Med*. 2020;26(6):909–918. doi:10.1038/s41591-020-0839-y
- Braun DA, Street K, Burke KP, et al. Progressive immune dysfunction with advancing disease stage in renal cell carcinoma. *Cancer Cell*. 2021;39(5):632–648.e638. doi:10.1016/j.ccell.2021.02.013
- Motzer RJ, Rini BI, McDermott DF, et al. Nivolumab for metastatic renal cell carcinoma: results of a randomized phase II trial. *J clin oncol*. 2015;33(13):1430–1437. doi:10.1200/JCO.2014.59.0703
- Wolock SL, Lopez R, Klein AM. Scrublet: computational identification of cell doublets in single-cell transcriptomic data. *Cell Systems*. 2019;8(4):281–291.e289. doi:10.1016/j.cels.2018.11.005
- Strack R. Afterglow probes made easy. *Nature Methods*. 2019;16(7):577. doi:10.1038/s41592-019-0483-y

30. Gulati GS, Sikandar SS, Wesche DJ, et al. Single-cell transcriptional diversity is a hallmark of developmental potential. *Science*. 2020;367(6476):405–411. doi:10.1126/science.aax0249
31. Qiu X, Mao Q, Tang Y, et al. Reversed graph embedding resolves complex single-cell trajectories. *Nature Methods*. 2017;14(10):979–982. doi:10.1038/nmeth.4402
32. Zheng C, Zheng L, Yoo JK, et al. Landscape of infiltrating T cells in liver cancer revealed by single-cell sequencing. *Cell*. 2017;169(7):1342–1356. e1316. doi:10.1016/j.cell.2017.05.035
33. Guo X, Zhang Y, Zheng L, et al. Global characterization of T cells in non-small-cell lung cancer by single-cell sequencing. *Nat Med*. 2018;24(7):978–985. doi:10.1038/s41591-018-0045-3
34. Oh DY, Fong L. Cytotoxic CD4+ T cells in cancer: expanding the immune effector toolbox. *Immunity*. 2021;54(12):2701–2711. doi:10.1016/j.immuni.2021.11.015
35. Glimcher LH, Townsend MJ, Sullivan BM, Lord GM. Recent developments in the transcriptional regulation of cytolytic effector cells. *Nat Rev Immunol*. 2004;4(11):900–911. doi:10.1038/nri1490
36. Brown DM, Lee S, Garcia-Hernandez M, Swain SL. Multifunctional CD4 cells expressing gamma interferon and perforin mediate protection against lethal influenza virus infection. *J Virol*. 2012;86(12):6792–6803. doi:10.1128/JVI.07172-11
37. Mucida D, Husain MM, Muroi S, et al. Transcriptional reprogramming of mature CD4+ helper T cells generates distinct MHC class II–restricted cytotoxic T lymphocytes. *Nat Immunol*. 2013;14(3):281–289. doi:10.1038/ni.2523
38. Reis BS, Rogoz A, Costa-Pinto FA, Taniuchi I, Mucida D. Mutual expression of the transcription factors Runx3 and ThPOK regulates intestinal CD4+ T cell immunity. *Nat Immunol*. 2013;14(3):271–280. doi:10.1038/ni.2518
39. Brown DM, Kamperschroer C, Dilzer AM, Roberts DM, Swain SL. IL-2 and antigen dose differentially regulate perforin- and FasL-mediated cytolytic activity in antigen specific CD4+ T cells. *Cellular Immunology*. 2009;257(1–2):69–79. doi:10.1016/j.cellimm.2009.03.002
40. Brown DM. Cytolytic CD4 cells: direct mediators in infectious disease and malignancy. *Cellular Immunology*. 2010;262(2):89–95. doi:10.1016/j.cellimm.2010.02.008
41. Sujino T, London M, Hoytema van Konijnenburg DP, et al. Tissue adaptation of regulatory and intraepithelial CD4 + T cells controls gut inflammation. *Science*. 2016;352(6293):1581–1586. doi:10.1126/science.aaf3892
42. Yasukawa M, Ohminami H, Arai J, Kasahara Y, Ishida Y, Fujita S. Granule exocytosis, and not the Fas/Fas ligand system, is the main pathway of cytotoxicity mediated by alloantigen-specific CD4+ as well as CD8+ cytotoxic T lymphocytes in humans. *Blood*. 2000;95(7):2352–2355. doi:10.1182/blood.V95.7.2352

## Publish your work in this journal

The Journal of Inflammation Research is an international, peer-reviewed open-access journal that welcomes laboratory and clinical findings on the molecular basis, cell biology and pharmacology of inflammation including original research, reviews, symposium reports, hypothesis formation and commentaries on: acute/chronic inflammation; mediators of inflammation; cellular processes; molecular mechanisms; pharmacology and novel anti-inflammatory drugs; clinical conditions involving inflammation. The manuscript management system is completely online and includes a very quick and fair peer-review system. Visit <http://www.dovepress.com/testimonials.php> to read real quotes from published authors.

Submit your manuscript here: <https://www.dovepress.com/journal-of-inflammation-research-journal>